Linear X-ray dichroism of cadmium sulphide with wurtzite and zincblende structures

1995 J. Phys.: Condens. Matter 7 2353

(http://iopscience.iop.org/0953-8984/7/11/014)

J. Phys.: Condens. Matter 7 (1995) 2353–2367. Printed in the UK

Linear x-ray dichroism of cadmium sulphide with wurtzite and zincblende structures

C Levelut†, Ph Sainctavit, A Ramos and J Petiau

Laboratoire de Minéralogie Cristallographie, CNRS URA9, Universités Paris 6 et 7, 4 Place Jussieu, 75252 Paris Cédex 05, France

Received 19 October 1994

Abstract. A comparison is made between x-ray absorption spectra at the sulphur K edge for CdS in wurtzite and zincblende structures. Differences between the polarization dependences of the x-ray spectra are expected due to the differences in symmetry for the two modifications. Multiple-scattering calculations in both structures are compared to published spectra and allow us to interpret a strong dichroic effect in the wurtzite structure. The intensity of a specific resonance is related to the middle-range order around sulphur atoms and potential applications of this fingerprint analysis are proposed.

1. Introduction

CdS doped glasses—and more generally many composites made of small semiconductor particles embedded in an insulating glass matrix—have recently been extensively studied, because of the reactivated interest in quantum confined semiconductors. This interest in spatial confinement of exciton or free carriers in one or more dimensions is motivated both by fundamental factors and for potential applications in non-linear optical devices. Three-dimensional confinement (quantum dots) can be produced in different solid dielectric matrices (glass, polymer, gel). The optical properties of such quantum dots differ from those of bulk material: they show discrete, large-molecular-like electronic states that shift towards higher energy with smaller particle sizes, leading to a blue shift of the optical absorption and large third-order susceptibility [1].

The average size of crystallites grown by diffusion controlled techniques can cover a wide range of values, from several micrometres down to a few ångströms, but the size distribution and quality of the interface with the dielectric differ from case to case. Only crystallites of II–VI and I–VII have been grown on glasses [2]. After the semiconductor clusters have grown beyond the nucleation stage, they acquire the crystalline structure and the stoichiometry of the bulk. For CdS, which can be obtained in the wurtzite or the zincblende structure, the nanocrystalline can *a priori* adopt either of the two structures. High-resolution transmission electron microscopy on CdS commercial glasses evidenced only wurtzite structure crystallites in the 1.5–10 nm range [3] while other studies attribute zincblende structure to crystallites smaller than 10 nm [4]. Other studies devoted to CdS in colloids indicate blende structure for small sizes (below 1–2 nm) and wurtzite for larger crystallites (greater than 5 nm) [5, 6]. For CdS doped materials, the shift of the exciton is

† Present address: Laboratoire de Science des Matériaux Vitreux, CNRS URA 1119 Université Montpellier II, Place Eugène Bataillon, 34095 Montpellier Cédex, France.

0953-8984/95/112353+15$19.50

pronounced for crystallites smaller than 6 nm. In this range of sizes, the crystallite structure is not well known and characterization by x-ray diffraction or high-resolution transmission electron microscopy is difficult. In this paper we show by multiple-scattering calculations that x-ray absorption spectroscopy is the suitable method to address this problem. Indeed although the local organization is very similar in both zincblende and wurtzite structures it is possible by a detailed examination of the polarization dependence of the absorption cross-sections to assign features to medium-range order (around 10 Å) and then to differentiate the two phases.

The aim of this paper is to exhibit the origin of dichroism and to discuss theoretically its importance. In the second section we outline the similarities and differences between the two modifications in which CdS can crystallize. The third section presents the theoretical background of multiple-scattering calculations with special attention to the questions of potential construction, symmetry and dichroism. The fourth section is devoted to the calculations of the isotropic spectra and to comparison with the experimental data, from which we infer the middle-range order information that can be extracted from x-ray absorption spectroscopy. In the fifth section the dichroic information is used to confirm the theory developed in the preceding section and the sixth section is a short conclusion.

2. Cadmium sulphide phases

CdS exists in two modifications with large similarities: zincblende and wurtzite. The zincblende structure can be described as two face centred cubic sublattices (one anionic and one cationic sublattice) shifted by $(\frac{1}{4}, \frac{1}{4}, \frac{1}{4})$ from one another [7]. The wurtzite structure is constituted by two hexagonal lattices (one anionic and one cationic sublattice) shifted by $(0, 0, u)$ [7]; u is a free parameter of the wurtzite structure and has the value 0.377 for CdS [8]. There exists an 'ideal' wurtzite structure where the hexagonal lattices are two compact hexagonal lattices ($c/a = \sqrt{3}/2\sqrt{2}$) with $u = \frac{3}{8}$ [7]. In both structures, the coordination shell of the anion is made up of four cations in tetrahedral symmetry and the second-neighbouring shell is made up of 12 anions. The electronic properties of the two phases are also rather similar: if the Brillouin zones are folded according to the axes of higher symmetry it can be shown that there exists a correspondence between the k vectors of the two Brillouin zones [9]. If the band structures are compared by using this correspondence, they are similar in shape, bandwidth and band gap [10].

X-ray absorption spectra at the sulphur K edge have been measured by Sugiura on powders for the two modifications [11]. It is found that the spectra are very similar. In the case of powder spectra, there is an angular averaging of the crystal orientations and no angular dependence can exist. Moreover since the first two neighbouring shells are for the two structures similar in nature and number but different for the angular arrangement of the second shell, any difference in the isotropic spectra can find two possible origins: a multiple-scattering process of higher order than single scattering in the first two shells or a multiple-scattering process (single scattering is included in multiple scattering) originating from beyond the second shell of neighbours. Both hypotheses lead to slight changes in the cross-section, as confirmed by experiment.

However, x-ray absorption performed on single crystals is a symmetry sensitive technique that should give different results for the two modifications of CdS. X-ray absorption spectra probe selectively any final states whose symmetries are determined by the electric dipole selection rules applied to the initial state. Indeed in the electric dipole approximation (valid at K edges for elements with $Z < 50$ [12]) the absorption cross-section

transforms under the action of rotations as a tensor of rank two [13]. For a crystal with cubic symmetry such as zincblende, there is no dependence of the x-ray absorption spectrum on the direction of polarization [14]. On the other hand, in the case of the wurtzite structure, the orientation group of the wurtzite space group is a hexagonal point group. In this case it has been shown that x-ray absorption spectra exhibit a dichroic dependence on the direction of the polarization vector. Then large differences are expected to occur for x-ray absorption spectra registered on single crystals with linear polarization.

3. Theoretical background

The x-ray absorption spectra have been calculated in the framework of the multiple-scattering method. The technique has already been extensively presented in numerous papers and its application to the case of x-ray absorption spectroscopy is the fruit of the pioneering work of J B Pendry and C R Natoli. There is no need to give much detail about the calculations since the essentials can be found elsewhere [15, 16]. Nevertheless we present three important points of the calculation: the construction of the potential, the reduction of the angular basis to a symmetrized one and the dichroic formalism. The potential is the central point in any multiple-scattering calculation and we shall give a precise description of its construction. The reduction of the angular basis set to a symmetrized basis set does not change the physics of the calculations except for the fact that, due to the large reduction of the secular determinant, it makes the calculations tractable for large clusters and large orbital momentum; this is not an easy matter and needs to be described in detail.

Theoretical calculations were performed for CdS at the K edge of sulphur with the multiple-scattering wave code developed by Natoli and coworkers, using the 'extended continuum' method [15, 16]. In this method advantage is taken of the fact that the electronic contribution to the cross-section can be fully separated from the geometrical part. The method is a real space method, where the absorption is calculated for a finite cluster of atoms. The absorbing atom is at the centre of the cluster and the cluster is constituted of the neighbouring shells around the absorbing atom. A shell is constituted of all the atoms at a same distance from the absorbing atom. The local point group of the absorbing sulphur atom in the cluster is the same as the local point group of the sulphur sites in the crystal. The absorption cross-section is proportional to the probability of transition from one core state to some continuum states and is given explicitly by the Fermi golden rule. The continuum states are expressed on the harmonic representation, which is a complete set of solutions of the Schrödinger equation. In this basis the cross-section can be expressed as

$$\sigma(\omega) = 4\pi^2\alpha\hbar\omega \sum_L |\langle\psi_{L,k}|\varepsilon \cdot r|\phi_i\rangle|^2 \frac{2mk}{\pi\hbar^2}$$

where α is the fine-structure constant, $\hbar\omega$ is the photon energy, k is the quantum momentum of the photoelectron such that $\hbar^2k^2/2m = h\omega - E_i$, ϕ_i is a solution of the Schrödinger equation for the initial state of binding energy E_i and $\varepsilon \cdot r$ is the interaction Hamiltonian in the electric dipole approximation. $\{\psi_{L,k}\}$ is a complete set of solutions of the Schrödinger equation; it is covered by k, which is a continuous index, and by a discrete compound index $L = (l, m)$. The coefficient $2mk/\pi\hbar^2$ finds its origin in the fact that the energy is expressed in Rydberg and k in atomic units so that $E = k^2$ and that the partial wave functions $\psi_{L,k}(r)$ have been normalized to one state per Rydberg: $\int_{\kappa_1}^{\kappa_2}\int_{\mathbb{R}^3} \psi^*_{L,k}(r) \cdot \psi_{L',k}(r)\,dr\,dk = \delta_{L,L'}$ (δ stands for the Kronecker index) where κ_1 and κ_2 are chosen so that $(\kappa_2)^2 - (\kappa_1)^2 = 1$.

3.1. Construction of the potential

For a given cluster we have to calculate the initial state and the complete set of final state wave functions. The initial state wave function is calculated by solving the Schrödinger equation in a spherical potential centred on the absorbing atom. The radius of the atomic sphere is somewhat arbitrarily determined and is usually set by following the so-called Norman prescriptions [17]. The Coulomb part of the potential is the atomic potential calculated from the self-consistent field (SCF) atomic wave functions tabulated by Clementi and Roetti [18]. An X–α exchange potential is added to this Coulomb potential [19] where the α parameter is the one recommended by Schwartz [20]. For a 1s state the radial Schrödinger equation is solved numerically for the experimental binding energy (2472 eV for the K edge of sulphur). It is checked that the radial wave function does not exhibit any divergence inside the muffin tin sphere of the absorbing atom due to a misadjustment of the binding energy. The 1s radial wave function of sulphur is not very sensitive to variations of the potential and it has been found that it does not lead to any relevant variation in the calculated spectra.

For the calculation of the final state wave functions, we apply the theory of multiple scattering in a muffin tin potential. Electronic atomic densities are calculated from self-consistent atomic potentials given by Clementi and Roetti [18]. The potential of the excited state is supposed to be a screened and relaxed potential: we select the $Z + 1$ atomic orbitals for the absorbing atom, remove a 1s electron (relaxation) and add an extra electron on the outer orbital to mimic screening of the hole. Around each atom, the tails of the electronic densities from the neighbouring atoms are superimposed on the SCF atomic electronic densities. The electronic density around each atom is spherically averaged and the Poisson equation is solved to produce the Coulomb part of the potential. To the Coulomb potential an exchange potential is added. It is an X–α potential given as a functional of the density previously calculated with the α parameter defined in the final state as for the initial state [20]. An energy dependent potential such as the complex Hedin–Lundqvist exchange and correlation potentials has been also tested and we do not present these results since calculations with the X–α or Hedin–Lundqvist potential gave very similar spectra in the first 10 eV above the edge [21]. This could be expected from the fact that the Hedin–Lundqvist potential is very similar to X–α for $k \approx 0$. Around each atom an atomic sphere is determined by fixing an atomic radius by the Norman criterion [17]: the charge enclosed in the atomic spheres has to be proportional to the atomic number Z of the atom enclosed and no overlap is considered. Inside each sphere the spherical part of the molecular potential (Coulomb and exchange potentials) is made spherically symmetric.

The cluster is surrounded by an outer sphere, which is the smallest sphere containing all the atomic spheres. Outside the outer sphere the potential is set to zero. Inside the outer sphere, we define the interstitial region as the region outside any atom and the potential in this region is set constant and equal to its volumic average. Since the cluster is usually large we consider that the net charge of the cluster is zero and no artificial charge is put on the surface of the outer sphere.

3.2. The symmetrized basis

We consider a cluster of N atoms, where the absorbing atom is at the origin. Inside each sphere the potential is spherically symmetric and the Schrödinger equation can be solved numerically for each partial wave $\psi_{L,k}(r)$. In the atomic sphere of the absorbing atom we can write:

$$\psi_{L,k}(r) = \sum_{L'} C_{L'}(L) R_{l'}(r) Y_{L'}(\hat{r})$$

where $Y_{L'}(\hat{r})$ are spherical harmonics and $R_{l'}(r)$ is the numerical solution regular at the origin of the radial Schrödinger equation. $C_{L'}(L)$ are a collection of parameters necessary to ensure the continuity of $\psi_{L,k}(r)$ and its first derivative.

In the interstitial region the potential is constant but its geometry is intricate. In a constant potential, any combination of spherical Bessel functions and spherical Neumann functions is solution of the Schrödinger equation. We consider that each function $\psi_{L,k}(r)$ in the interstitial region can be expressed as

$$\psi_{L,k}(r) = j_{l'}(kr)Y_{L'}(\hat{r}) - i\sum_{nL'} B^n_{L'}(L)t^n_{l'}h_{l'}(kr_n)Y_{L'}(\hat{r}_n)$$

where $j_{l'}(kr)$ are spherical Bessel functions centred on the absorbing atom and $h_{l'}(kr_n)$ are Hankel functions centred at atomic site n; $t^n_{l'} = \sin\delta^n_{l'}\exp(\delta^n_{l'})$ where $\delta^n_{l'}$ are the atomic scattering phase shifts of the atom n. In the summation n runs from one to N (total number of atoms in the cluster) and l' from zero to infinity.

The parameters $B^n_{L'}(L)$ are determined by imposing continuity conditions for the partial wave $\psi_{L,k}(r)$ and its first derivative at the border of the atomic spheres. In doing so the normalized partial wave $\psi_{L,k}(r)$ is exactly determined inside the atomic sphere of the absorbing atom. The cross-section is then a sum of terms of the type $|\langle\psi_{L,k}|\varepsilon\cdot r|\phi_i\rangle|^2$ where the integral is only to be performed inside the atomic sphere of the absorbing atom since the radial part of $\phi_i(r)$ is almost zero if r is larger than a few tenths of an ångström.

Inside the atomic spheres and in the interstitial region, the angular basis set is the set of spherical harmonics $Y_L(\hat{r})$. In all the expressions above there is a summation up to infinity over the discrete compound index $L = (l, m)$. In the calculations, the summation is truncated to a certain $l_{\max}$ whose value is determined by the rule of thumb $l_{\max} > R_{m.t.}k$. Indeed by analogy with $j_l(kr)$, which is negligible for $kr < \sqrt{l(l+1)}$, we assume that the radial wave function solution of the radial Schrödinger equation in one specific atomic sphere will behave in the same way. Then there is no need to extend the summation beyond $l_{\max}$ since the solution R and the corresponding phase shift are almost zero. Each function $\psi_{L,k}(r)$ is extended on a finite set of basis functions that are the spherical harmonics centred on the different atoms for $l = 0$ up to $l = l_{\max}$. If every sphere has the same $l_{\max}$ there are $N(l_{\max}+1)^2$ different angular functions. It can be easily shown that to satisfy the multiple-scattering equations the coefficients $B^n_{L'}(L)$ have to satisfy the following vectorial equations:

$$B(L) = [\mathbf{T}^{-1} - \mathbf{G}]^{-1}J(L)$$

and

$$B(L) = -C(L)$$

where the vectors $B(L)$ and $C(L)$ are defined by $[B(L)]_\alpha = B_\alpha(L)$ and $[C(L)]_\alpha = C_\alpha(L)$ and the matrix $\mathbf{T}$ is the diagonal matrix defined by $[T]_{\alpha,\beta} = \delta_{n',n''}\delta_{l',l''}\delta_{m',m''}t^{n'}_{l'}$ with the compound index $\alpha = \{n';(l',m')\}$. The $[G]_{\alpha,\beta}$ matrix, also called the propagator, and the $[J]_\alpha$ vector are related to the translation operator in the harmonic representation. These are geometric quantities independent of the potential, whose calculation is tedious but straightforward for any cluster geometry. The translation operator is an irreducible tensor of rank one of the group of rotations SO(3) [22, 23]. It then transforms like the totally symmetric irreducible representation of any point group.

If **g** is the local point group that leaves the cluster invariant, it can be shown that the matrices associated with the transformation of the $N(l_{max}+1)^2$ angular basis functions (spherical harmonics) under the operations of the group **g** constitute a representation of **g** with the dimension $N(l_{max}+1)^2$. This representation, labelled Γ, can be decomposed into a sum of irreducible representations: $\Gamma = \oplus_i n_i \Gamma_i$ where Γ_i is the ith irreducible representation of **g**, which appears n_i times in the decomposition of Γ. There is a unitary transformation that transforms the angular basis set $\{Y_L(\hat{r}_i)\}$ into a new basis set $\{\phi\}$ in which each element transforms like one basis partner of an irrep of **g**. The new basis set is constructed by the use of the projection operators, associated with the irreps of **g** [24]. The new basis set $\{\phi_{i,m,q}\}$ can be labelled by three indices as follows: $\phi_{i,m,q}$ is the qth partner of the mth basis of irrep Γ_i. The ranges of variation for the indices are $1 \leqslant q \leqslant d^i$ where d^i is the dimension of Γ_i and $1 \leqslant m \leqslant n_i$ where n_i is the multiplicity of Γ_i in Γ. If **O** is an irreducible tensor of rank one in SO(3), the Wigner–Eckhart theorem for finite groups states that $\langle \phi_{i,m,q} | \mathbf{O} | \phi_{j,n,q} \rangle = \delta_{i,j}\delta_{q,p}\langle \Gamma^i_m \parallel \mathbf{O} \parallel \Gamma^i_n \rangle$. It can be shown that the $[G]_{\alpha,\beta}$ matrix can be expressed as $\langle \phi_\alpha | \mathbf{O} | \phi_\beta \rangle$ with $\alpha = (i, m, q)$ where **O**, the transitional operator for Hankel functions, is an irreducible tensor of rank one. In the basis $\{\phi_{i,m,q}\}$ **G** is block diagonal if the functions $\{\phi_{i,m,q}\}$ are ordered by first running m, then q and then i. The dimension of the block is n_i, the multiplicity of Γ_i in the representation Γ. Moreover the submatrices related to any partner of one given representation are all the same. Since the transition matrix **T** is still diagonal in $\{\phi_{i,m,q}\}$, the matrix $[\mathbf{T}^{-1} - \mathbf{G}]$ is block diagonal too and can be inverted by block: there is no admixture of matrix elements related to different irreps or different partners of the same irrep. The case of wurtzite and zincblende is developed in the appendix. We want to point out that in the subset of symmetry allowed basis functions (the set of basis function belonging to the same irrep) the only parameters $B^n_{L'}(L)$ present in the cross-section are those for which the corresponding basis is built of $l' = 1$ spherical harmonics. Nevertheless the secular equation with the complete subset has to be calculated because $[\mathbf{T}^{-1} - \mathbf{G}]$ is only block diagonal for this subset.

3.3. Linear dichroism

The dependence of the x-ray absorption spectra on polarization direction in the case of linearly polarized light has been extensively detailed by Brouder [13]. The local point group for the anionic and cationic sites is $T_d(\bar{4}3m)$ in the zincblende structure and C_{3v} ($3m$) in the wurtzite structure.

In symmetry T_d, the electric dipole selection rule applied to a K shell gives that the only $B_{L'}(L)$ that need to be known are those for which the angular part transforms like one partner of the Γ_5 irrep: we have chosen those that transform like x (we use Koster notations for point group irreps) [25]. In the case of zincblende the cross-section is isotropic and no polarization dependence exists.

In symmetry C_{3v}, the electric dipole selection rules state that there are two groups of $B_{L'}(L)$ that need to be known: the one for which the corresponding angular part transforms like Γ_1 and the one for which the corresponding angular part transforms like one partner of the two-dimensional irrep Γ_3 (we have chosen the ones that transform like x). Two cross-sections are calculated separately, $\sigma_\perp$ for the x polarization and $\sigma_\parallel$ for the z polarization. In the wurtzite crystal, the absorption cross-section is dichroic and any spectrum can be expressed as a linear combination of the two spectra $\sigma_\parallel$ and $\sigma_\perp$. The coefficients of the linear combination are geometric coefficients independent of the material and only related to the orientation of the polarization vector. This result is valid on the whole energy range of x-ray absorption spectra as long as the electric dipole approximation is valid. The absorption

cross-section for a polarization vector that makes an angle θ with the ternary axis can be expressed by separating the isotropic and non-isotropic parts of the cross-section [13]:

$$\sigma(\theta) = \cos^2\theta\sigma_{\parallel} + \sin^2\theta\sigma_{\perp}$$

or

$$\sigma(\theta) = \sigma_{\text{powder}} - (1/\sqrt{2})(3\cos^2\theta - 1)\Delta\sigma$$

where σ_{powder} is the isotropic absorption cross-section for a powder spectrum and $\Delta\sigma$ is the non-isotropic contribution: $\sigma_{\text{powder}} = \frac{1}{3}(2\sigma_{\perp} + \sigma_{\parallel})$ and $\Delta\sigma = (\sqrt{2}/3)(\sigma_{\perp} - \sigma_{\parallel})$.

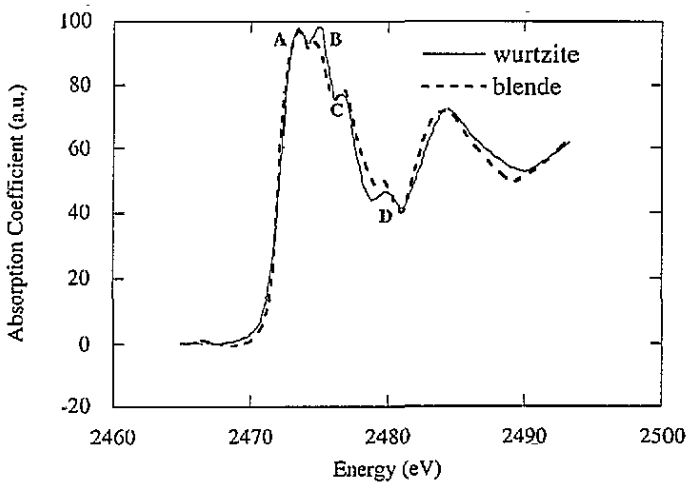

Figure 1. Experimental spectra recorded at the sulphur K edge by Sugiura [11] for CdS powders with zincblende and wurtzite structures.

4. Isotropic sulphur K edge spectra

Sugiura has recorded spectra on CdS of both zincblende and wurtzite structures at the K edge of sulphur [11] (figure 1). The two spectra are isotropic spectra that have been recorded on powder samples. They are much alike except for small differences: the B resonance has a higher intensity in the wurtzite structure than in the zincblende structure and the D resonance is higher for the zincblende structure than for the wurtzite structure. The relative positions of the B and C resonances for the two structures are strongly dependent on the normalization conditions chosen to compare the two experimental spectra and moreover the differences are small for the feature C. Then we consider that the only relevant important difference between zincblende and wurtzite isotropic spectra at the sulphur K edge is related to the intensity and energy of resonance D. This will be the central point of our discussion.

The multiple-scattering calculations for CdS in the zincblende structure are performed with the crystal parameter $a = 4.12_4$ Å [8]. For CdS in the wurtzite phase, we assume an 'ideal' wurtzite structure ($u = \frac{3}{8}$ and $c/a = \sqrt{3}/2\sqrt{2}$) with $c = 6.73_5$ Å [7]. In doing so,

the coordination shell is a perfect tetrahedron of cadmium atoms and the second shell is made up of 12 sulphur atoms situated at exactly the same distance from the central sulphur atom. In wurtzite and in zincblende structures the first two shells are then constituted of the same number of atoms of the same nature and at the same distance although the angular distribution is different [26]. The zero of energy of the calculations is the vacuum level of the crystal. In CdS it is rather independent of the structure and located 10 eV higher in energy than the interstitial muffin tin potential. The calculated spectra are convoluted by a Lorentzian function whose width at half maximum is related to the effective mean free path of the photoelectron, which takes into account the experimental resolution (0.2 eV), the finite lifetime of the core hole (0.5 eV) and the inelastic scattering of the photoelectron with the electrons of the material.

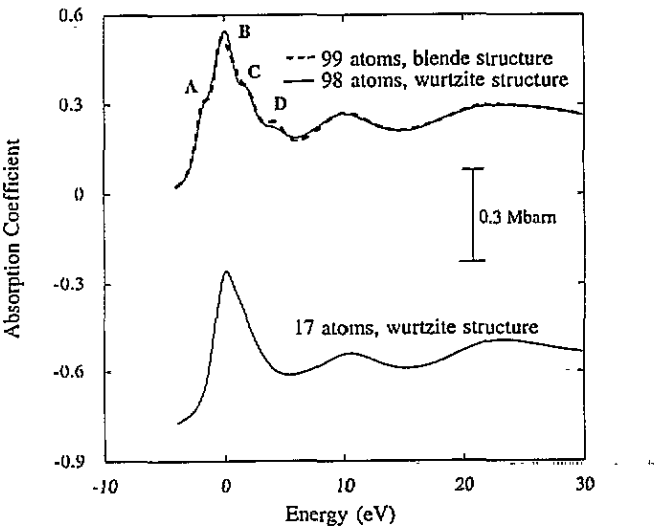

Figure 2. Calculated spectra of zincblende and wurtzite CdS at the sulphur K edge; 17-atom clusters (for wurtzite only) and ~ 100-atom clusters.

In both structures, the main resonances are present for a two-shell cluster calculation (figure 2). However, the resonances show strong evolution in their positions, intensities and shapes when the size of the cluster is increased. We find that convergence is obtained for both structure calculations when the cluster size is around 100 atoms (figure 2). This corresponds to eight shells in zincblende with 99 atoms and a cluster diameter equal to 18.5 Å while in the wurtzite structure it is a 13-shell cluster (98 atoms) with diameter 18.5 Å. Although the cluster is large, it is possible to determine the specific contribution of the particular shells. Indeed a focusing effect is present when two neighbouring shells are collinear with the absorbing atom. Due to large forward scattering for any photoelectron energy, the contribution of a distant shell is enhanced by the relay of the intermediate one. This is what happens for the eighth shell of the zincblende cluster (12 sulphur atoms) that contributes highly to the cross-section due to the collinearity with the second shell. In the wurtzite cluster the 13th shell (six sulphur atoms in the plane perpendicular to c) is collinear with six out of the 12 second neighbours and the focusing effect is less important than for zincblende on the isotropic spectrum although it is very strong for $\sigma_\perp$.

In figure 2, the isotropic calculated spectra are almost the same for zincblende and wurtzite structures except for a few differences: the B resonance has a higher intensity for the wurtzite structure and the D resonance is much higher for the zincblende structure. For both structures, the experimental and calculated spectra presented in figures 1 and 2 are quite similar for a large enough cluster ($\sim$ 100-atom clusters). The main difference originates from the intensity of resonance A that is much higher in the experimental spectra for both phases than in the calculated spectra.

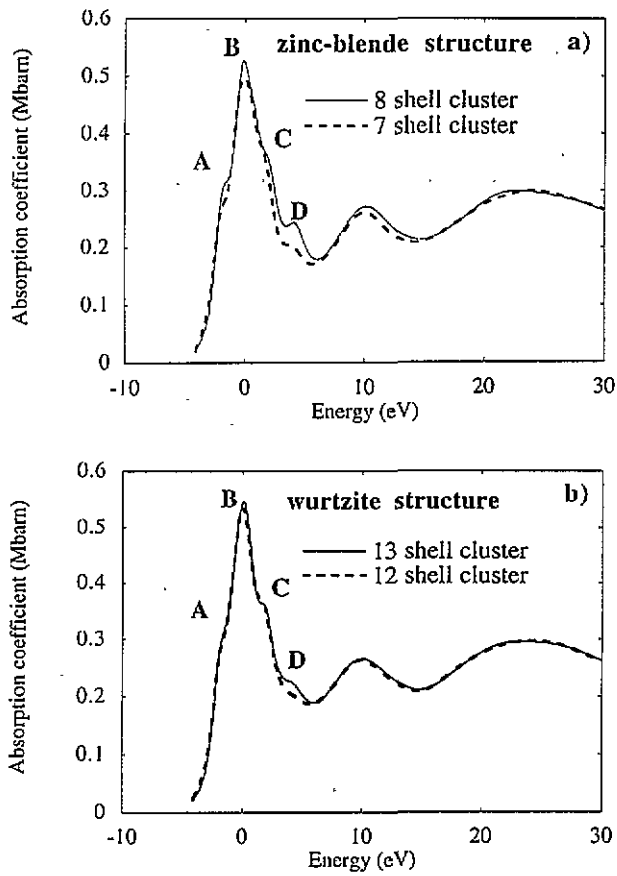

Figure 3. Calculated spectra at the sulphur K edge for CdS. (a) The zincblende structure, for a seven-shell (87-atom) cluster and an eight-shell (99-atom) cluster. The shell added between the two calculations is constituted of 12 sulphur atoms at 8.25 Å from the absorbing atom. (b) Isotropic spectra in the wurtzite structure, for a 12-shell (92-atom) cluster and a 13-shell (98-atom) cluster. The added shell contains six sulphur atoms at 8.25 Å from the absorbing atom.

For the zincblende structure, the addition of the eighth shell strongly enhances the D resonance (figure 3). For the wurtzite structure, the D resonance is also enhanced when the 13th shell is taken into account (figure 3). In both phases, the added shells (sulphur atoms at $\sim$ 8.25 Å) contribute to a focusing effect. Figure 4 shows the difference signal between the 13- and the 12-shell clusters in the wurtzite structure. For the difference process, the raw calculated spectra are subtracted without energy shift to take into account

any modifications of the zero energy. In doing so we do not introduce any adjustable parameter but are very sensitive to slight modifications (0.01 eV) of the interstitial muffin tin potential, which depends on the atomic nature of the cluster outer shell. This is the origin of the large non-physical derivative signal that is seen between −5 eV and 2 eV. In the energy region from 3 to 5 eV (resonance D) the addition of the 13th shell induces an enhancement of the D resonance. Although the previous derivative signal (from −5 eV to 2 eV) is very sensitive to any energy shift, the difference signal at resonance D is broad and constant. By the difference method between the calculated spectra of wurtzite, we have pinned the importance of the eighth shell in the origin of the D resonance where collinearity and focusing effect are certainly of importance, but the types of path to which this shell is contributing in the scattering process are not clear and cannot be addressed by *full* multiple-scattering calculations.

The difference between the eight- and seven-shell clusters in the zincblende structure is also plotted in figure 4 and similar conclusions relative to the influence of the eighth shell on the appearance of the D resonance can be drawn. This strongly expresses the fact that the isotropic spectra of the two phases are governed by the same laws.

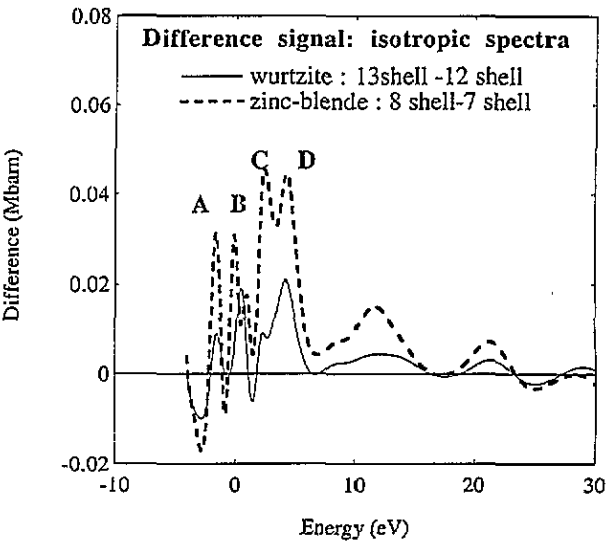

Figure 4. The difference signal between the isotropic spectra for the 13-shell cluster and the 12-shell cluster of the wurtzite structure. A comparison with the difference signal between the spectra for the eight-shell cluster and the seven-shell cluster in the zincblende CdS.

5. Dichroism at the sulphur K edge

Figure 5 compares the difference signal for $\sigma_{\parallel}$ between the 13- and the 12-shell clusters in the wurtzite structure and the difference signal for $\sigma_{\parallel}$ between the eight- and the seven-shell clusters in the zincblende structure. At the energy of resonance D there is no contribution to the difference signal for the wurtzite structure. This originates from the fact that the six sulphur atoms of the 13th shell are located in the plane perpendicular to the c axis. From

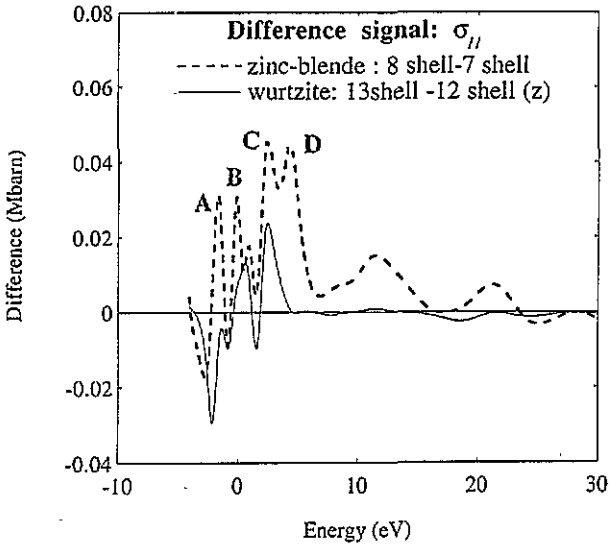

Figure 5. The difference signal for $\sigma_{\parallel}$ between the 13- and 12-shell clusters in the wurtzite structure. A comparison with the difference signal for $\sigma_{\parallel}$ between the spectra for the eight-shell cluster and the seven-shell cluster in the zincblende structure.

the very simplified theory of single scattering in the plane approximation [27], it can be inferred that the contribution to the cross-section due to the six sulphur atoms is zero since there is 90° between the polarization vector and the vector joining the absorbing atom to any of the sulphur atoms from the 13th shell. This argument can be refined to the case of full multiple-scattering calculations. The 13th shell is made up of six sulphur atoms and 64 angular basis functions can be constructed with the condition $0 \leqslant l \leqslant 3$. For $l \geqslant 3$ the phase shifts are almost zero for photoelectron energy less than 10 eV as is the case for resonance D. For the calculation of $\sigma_{\parallel}$ the angular functions of the symmetrized basis set transform like the one-dimensional irrep Γ_1 of C_{3v}. There are six such basis functions for $l \leqslant 3$ out of a total of 299 symmetrized basis functions for the whole 13-shell cluster: one with $l = 1$, two with $l = 2$ and three with $l = 3$. The inspection of the phase shifts δ_l shows that for $l > 2$ δ_l is very close to zero. This means that the scattering efficiency of the 13th shell is low since the number of basis functions that carry the scattering amplitude $t_{l'}$ is 1% of the total number of basis functions: the focusing effect is still present since it is a geometrical condition, but it is not efficient in the case of the polarization vector parallel to c.

The difference between the eight- and seven-shell clusters in the zincblende structure is also plotted in figure 5. The equivalent of $\sigma_{\parallel}$ is obviously σ_{iso} since zincblende is cubic and the conclusions of the previous section apply to this case: a focusing effect is responsible for an increase of the intensity of resonance D.

Figure 6 shows the absorption cross-section when the polarization vector is along the x direction for a 13-shell cluster in the wurtzite structure. From geometrical considerations, one expects that resonance D is much increased by the adjunction of the 13th shell in the cluster. Following again simple but useful arguments based on single scattering in the plane wave approximation one can estimate the apparent number of the six planar atoms. It is given by $N = \sum \cos^2 \theta$ where θ is the angle between the polarization vector and the vector joining the central atom and any of the six neighbouring atoms. We find $N = 9$, which

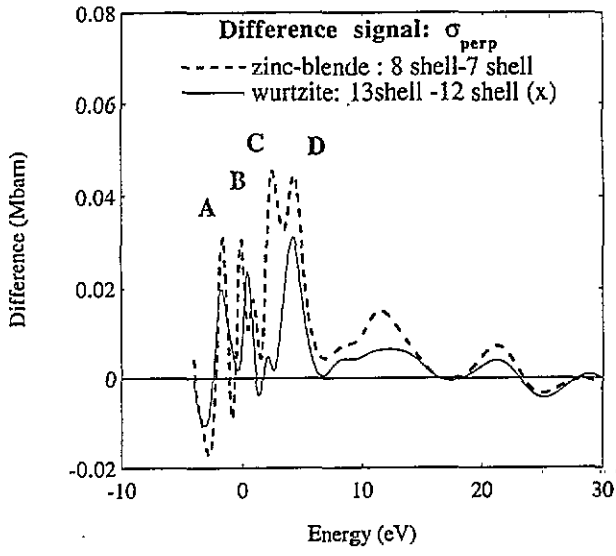

Figure 6. The difference signal for $\sigma_\perp$ between the 13- and 12-shell clusters in the wurtzite structure. A comparison with the difference signal for $\sigma_\perp$ between the spectra for the eight-shell cluster and the seven-shell cluster in the zincblende structure.

means that the weight of the six atoms of the 13th shell in $\sigma_\perp$ is 50% greater than it is in the isotropic spectrum. A careful look at the symmetrized basis set shows also that the shell contributes significantly to the cross-section: 21 angular functions transforming like the first partner of the two-dimensional irrep Γ_3 out of 521 basis functions: two for $l = 0$, five for $l = 1$, six for $l = 2$ and eight for $l = 3$. In the same way as for $\sigma_\parallel$ the phase shifts for $l = 3$ are small and only slightly contribute to the cross-section, but unlike the $\sigma_\parallel$ case the contribution of the 13 basis functions for $l \leqslant 2$ is large (2.5% of the total basis set). Thus we find that our analysis clearly points out that resonance D mainly finds its origin in the 13th shell, whose influence is enhanced by collinearity. In the isotropic spectrum the resonance D is also enhanced by the presence of the 13th shell since $\sigma_\perp$ weights 67% of the isotropic spectrum.

The difference signal for the x polarized cross-section between the 13- and the 12-shell clusters in the wurtzite structure is compared in figure 6 to the difference between the eight- and seven-shell clusters in the zincblende structure. The enhancement of the D resonance in the case of the wurtzite structure is a little more than three-quarters of the enhancement for the zincblende structure (if the areas of the peaks are measured). This is in complete agreement with the attribution of resonance D to the focusing effect. Indeed in zincblende there are 12 atoms in the eighth shell that can benefit from the focusing effect while in $\sigma_\perp$ of wurtzite the apparent number of atoms from the 13th shell is nine.

Although in the wurtzite structure the 11th shell (twelve sulphur atoms) is twice as large as the 13th shell and at a similar distance from the central atom (7.90 Å against 8.25 Å), there is evidence from our calculations that it does not greatly contribute to any specific feature but only modifies the cross-section by a few percent. The origin of the effect is to be found in the large distance between the 11th shell and the central atom and in the absence of focusing geometry.

6. Conclusion

In this paper we have addressed the important question of the determination of the geometrical environment of sulphur in either wurtzite or zincblende cadmium sulphide. We have shown that there exists a signature of the two phases that is present in the x-ray absorption spectra at the sulphur K edge. This signature is related to the intensity of resonance D, which is due to the presence of the eighth shell in the zincblende structure or to the 13th shell in the wurtzite structure. These two shells are constituted of sulphur atoms at 8.25 Å, all collinear to the atoms of the second shell of neighbours. This D resonance is characteristic of a middle-range order and its intensity has been shown to be proportional to the number of atoms in the eighth or in the 13th shell.

This finding receives two possible applications. Firstly it can be applied to the phase determination of large crystallites when other methods such as x-ray diffraction or high-resolution transmission electron microscopy are not tractable. This result is essential since EXAFS cannot unambiguously distinguish between the two phases. Indeed although in the wurtzite phase the second shell of neighbours around sulphur atoms contains a cadmium atom, the contribution of this cadmium is very small due to a relatively small scattering amplitude in the intermediate energy range (3–6 $Å^{-1}$).

Secondly if the phase (wurtzite or zincblende) of small crystallites can be determined, one can extract their sizes from x-ray absorption data. For small crystallites of CdS in silicate glasses, the intensity of resonance D in sulphur K edge spectra is characteristic of the atomic shell located at 8.25 Å from the absorbing atom. One can use the intensity of D to determine the proportion of sulphur atoms having one or several eighth or 13th neighbours. This can then be related to the size of the crystallites, if complementary information is known by other techniques (for example the shapes of the crystallites). High-resolution transmission electron microscopy [3] shows that the crystallites have hexagonal shapes. If we consider a small hexagonal crystallite of 8.25 Å radius, there are seven atoms with six 13th neighbours, and six atoms with two 13th neighbours in the section of the crystallite instead of 19 atoms with six 13th neighbours in a bulk crystal. So the intensity of the D resonance should be equal to half the intensity of the D resonance for a bulk crystal of wurtzite structure.

Full multiple-scattering calculations are not the only way of extracting information from XAS data. Path analysis as developed by several authors [28, 29] has proved to be very valuable for understanding middle-range order by a thorough multiple-scattering analysis of the EXAFS region. Nevertheless it has also been shown that this approach could face divergence close to the edge for low-Z atoms such as sulphur or silicon atoms, which could prevent an analysis of the first empty states above the Fermi level. In such cases full multiple-scattering calculations are found to be the proper method of investigation.

Appendix. Basis symmetrization for zincblende and wurtzite structures

In order to illustrate what has been said in the section on symmetry, we apply the symmetrization method to the case of the zincblende structure. In the zincblende crystal the local point group of the sulphur site is $T_d(\bar{4}3m)$. To T_d correspond five irreps: two one-dimensional irreps, one two-dimensional irrep and two three-dimensional irreps. Then it follows from the Wigner–Eckhart theorem for finite groups that in the symmetrical basis $\{\phi_{i,m,q}\}$, the matrix $[\mathbf{T}^{-1} - \mathbf{G}]$ is block diagonal with 10 blocks, where the block $\mathbf{H}_i$ is an

n_i-dimensional matrix where n_i is the multiplicity of Γ_i in Γ. The matrix $\mathbf{H}_i$ appears d_i times where d_i is the dimension of irrep Γ_i.

$$\begin{vmatrix} \mathbf{H}_1 & & & & & & & & & \\ & \mathbf{H}_2 & & & & & & & \mathbf{0} & \\ & & \mathbf{H}_3 & & & & & & & \\ & & & \mathbf{H}_3 & & & & & & \\ & & & & \mathbf{H}_4 & & & & & \\ & & & & & \mathbf{H}_4 & & & & \\ & & & & & & \mathbf{H}_4 & & & \\ & & & & & & & \mathbf{H}_5 & & \\ & \mathbf{0} & & & & & & & \mathbf{H}_5 & \\ & & & & & & & & & \mathbf{H}_5 \end{vmatrix}.$$

For a K edge in T_d symmetry, the initial state transforms like Γ_1 and the Hamiltonian interaction transforms like an irreducible tensor of Γ_5 (we follow Koster notations). The dipole allowed final states have to transform like Γ_5 and it is sufficient to retain in the basis set the basis functions that transform like one given partner (usually the partner x) of Γ_5. The other basis functions can be discarded and the full matrix to invert is no longer $[\mathbf{T}^{-1} - \mathbf{G}]$ but $[\mathbf{H}_5]$. Since the $[\mathbf{T}^{-1} - \mathbf{G}]$ matrix is constituted of ten blocks and, for a large basis set, each block has more or less the same dimension, the dimension of matrix $[\mathbf{H}_5]$ is on average 10 times smaller than that of $[\mathbf{T}^{-1} - \mathbf{G}]$. This corresponds to a huge economy of time, since the inversion of matrix $[\mathbf{T}^{-1} - \mathbf{G}]$ varies as the cube of its dimension. We found that for large clusters and large l_{max} the dimension of $\mathbf{H}_5$ is around 15% of the dimension of $\mathbf{G}$ and the CPU time is divided by 400. By completely using the symmetry of the cluster it is then possible to perform calculations for large clusters ($\sim$ 150 atoms) with an extended basis ($l_{max} = 6$) in reasonable times.

The application of the symmetrization method to the case of the wurtzite structure is similar although somewhat more complicated due to the lower symmetry of the sulphur atomic site. In the wurtzite crystal the local point group of the sulphur site is $C_{3v}(3m)$. To C_{3v} correspond three irreps: two irreps of dimension one and one of dimension two. Then it follows from the Wigner–Eckhart theorem for finite groups that in the symmetrized basis $\{\phi_{i,m,q}\}$, the matrix $[\mathbf{T}^{-1} - \mathbf{G}]$ is block diagonal with four blocks.

$$\begin{vmatrix} \mathbf{H}_1 & & & \mathbf{0} \\ & \mathbf{H}_2 & & \\ & & \mathbf{H}_3 & \\ \mathbf{0} & & & \mathbf{H}_3 \end{vmatrix}.$$

For a K edge in C_{3v} symmetry, the initial state transforms like Γ_1 and the Hamiltonian interaction transforms like the irreducible tensors of Γ_1 (ϵ parallel to z) and Γ_3 (ϵ perpendicular to z). The dipole allowed final states have to transform like Γ_1 or Γ_3 and the calculation can be divided into two parts. Firstly, when ϵ is parallel to z, the basis functions are the functions that transform like Γ_1 and the matrix to invert is of the same size as $\mathbf{H}_1$, and secondly, when ϵ is perpendicular to z, the basis functions are the functions that transform like one partner (usually x) of Γ_2 and the matrix to invert is of the same size as $\mathbf{H}_2$. The gain on the calculation time due to the basis reduction is not as important as for the case of zincblende but can be estimated as a factor of 20.

References

[1] Flytzanis C 1975 *Quantum Electronics: A Treatise* vol 1a, ed H Rabin and C L Tang (New York: Academic)
[2] Ekimov A I, Onushchenko A A and Tsekhomskii V A 1980 *Fiz. Khim. Stekla* 6 511
[3] Allais M and Gandais M 1990 *J. Appl. Crystallogr.* **23** 418
[4] Ekimov A I, Efros AL L, Ivanov M G, Onushchenko A A and Shumilov S K 1989 *Solid State Commun.* **69** 565
[5] Rossetti R, Ellison J L, Gibson J M and Brus L E 1984 *J. Chem. Phys.* **80** 4464
[6] Weller H, Schmidt H M, Koch U, Fotjik A, Baral S, Henglein A, Kunath W, Weiss K and Dieman E 1986 *Chem. Phys. Lett.* **124** 557
[7] Roth W L 1967 *Physics and Chemistry of II–VI compounds* (Amsterdam: North-Holland)
[8] Stevenson A W and Barnea Z 1984 *Acta Crystallogr.* B **40** 521
[9] Birman J L 1959 *Phys. Rev.* **115** 1493
[10] Chang K J, Froyen S and Cohen M L 1983 *Phys. Rev.* B **28** 4736
[11] Sugiura C 1971 *J. Phys. Soc. Japan* **31** 6
[12] Müller J E and Wilkins J W 1984 *Phys. Rev.* B **29** 4331
[13] Brouder C 1990 *J. Phys.: Condens. Matter* **2** 701
[14] Nye J F 1957 *Physical Properties of Crystals* (Oxford: Clarendon)
[15] Natoli C R, Misemer D K, Doniach S and Kutzler F W 1980 *Phys. Rev.* A **22** 1104
[16] Natoli C R, Benfatto M and Doniach S 1986 *Phys. Rev.* A **34** 4682
[17] Norman J G Jr 1976 *Mol. Phys.* **31** 1191
[18] Clementi E and Roetti 1974 *At. Data Nucl. Data Tables* **14** 183
[19] Slater J C and Johnson K H 1972 *Phys. Rev.* B **5** 844
[20] Schwartz K 1972 *Phys. Rev.* B **5** 2466
[21] Hedin L and Lundqvist B I 1969 *Solid State Physics* vol 23 (New York: Academic) p 1
[22] Cornwell J F 1990 *Group Theory in Physics (Techniques in Physics 7)* ed N H March (New York: Academic)
[23] Weissbluth M 1978 *Atoms and Molecules* (New York: Academic–Harcourt Brace Jovanovich)
[24] Tinkham M 1964 *Group Theory and Quantum Mechanics* (New York: McGraw-Hill)
[25] Koster G F, Dimmock J O, Wheeler R G and Statz H 1966 *Properties of the Thirty-two Point Groups* (Cambridge, MA: MIT Press)
[26] Lawaetz P 1972 *Phys. Rev.* B **5** 4039
[27] Heald S M and Stern E A 1977 *Phys. Rev.* B **16** 5549
[28] Rehr J J and Albers R C 1990 *Phys. Rev.* B **41** 8139
[29] Filipponi A, Di Cicco A, Tyson T A and Natoli C R 1991 *Solid State Commun.* **78** 265